PHYSICAL REVIEW
LETTERS

VOLUME 22 | 10 MARCH 1969 | NUMBER 10

# LEVEL-CROSSING SPECTROSCOPY IN MOLECULES: APPLICATION TO THE OH FREE RADICAL*

A. Marshall, R. L. deZafra, and Harold Metcalf
Department of Physics, State University of New York, Stony Brook, New York 11790
(Received 15 January 1969)

We have observed the Hanle effect in the $^2\Sigma$ ($v=0$) excited state of the free radical OH in lines which originate from sublevels with rotational quantum numbers $K=3,4,5$. From the widths of each of these experimental signals we can calculate the $g$-factor–lifetime product and, since the lifetime of the state has been measured previously, our observations yield the values $g[K=3]=0.176(23)$, $g[K=4]=0.141(15)$, and $g[K=5]=0.118(11)$.

Recently Zare has explored the theory of level-crossing spectroscopy as applied to molecular systems[1] and has used the Hanle effect (zero-field level crossing) to determine the $g$ factor experimentally and set an upper limit for the $\rho$-doubling constant in the $^2\Sigma^+$ electronic excited state of the NO molecule.[2]

We report here a study of the Hanle effect in the free radical OH which yields measurements of the $g$ factors for a set of rotational sublevels within the $^2\Sigma^+$ ($v=0$) electronic excited state. From these $g$ factors some deductions may be made concerning the coupling in the $^2\Sigma$ state.

The electronic ground state of the hydroxyl radical is a $^2\Pi$ configuration. Each of its vibrational levels is subdivided into various rotational sublevels, designated by the quantum number $K$, which are in turn further split by both $\Lambda$ doubling and the hyperfine interaction. The rotational structure of the $^2\Sigma^+$ excited state is split by $\rho$ doubling and the hyperfine interaction.[3] Transitions from levels of the $^2\Sigma^+$ complex to levels of the ground configuration give rise to the well-known uv band in the OH spectrum, with its head at 3068 Å. (This system has been extensively catalogued in the definitive work on the OH spectrum by Dieke and Crosswhite,[4] and we use their notation throughout this paper.) Our measurements to data have been confined to $^2\Sigma$ ($v=0$) rotational levels for which $K=3$, 4, and 5.

The Hanle effect manifests itself as a change in the angular distribution of fluorescence in the vicinity of zero magnetic field where the Zeeman components of the excited state become degenerate. With the fixed orthogonal geometry shown in Fig. 1, the fluorescent intensity at the detector, as a function of magnetic field $H$, is a Lorentzian line shape given by an equation of the form[1,5]

$$I = I_0\{1 \pm [1 + (2g\mu_0 H\tau/\hbar)^2]^{-1}\} + \text{const}, \qquad (1)$$

where $g$ and $\tau$ are, respectively, the $g$ factor and

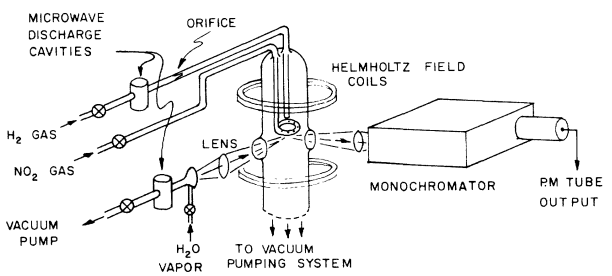


FIG. 1. Schematic diagram of the experimental arrangement. Input, output, and $H$-field axes are mutually orthogonal.

the mean life for the radiating state and $\mu_0$ is the Bohr magneton. The field $H_{1/2}$ required to produce the half-maximum signal amplitude is hence given by the relation

$$g\tau = \hbar/2\mu_0 H_{1/2}. \quad (2)$$

Since the quantities on the right are readily evaluated, the product $g\tau$ may be experimentally determined.

A major difficulty occurring in the application of the level-crossing technique to molecules is caused by the multitude of closely spaced rotational levels, which may be further split by small effects such as $\rho$ and $\Lambda$ doubling and the hyperfine interaction. In practice one may be unable to separate light scattered from several adjacent sublevels belonging to one or more rotational states. The resultant conglomeration will typically show a very weak level-crossing signal (e.g., $\lesssim 1$ % of the scattered light) compared with as high as 100% in the well-separated atomic transitions studied previously. In their pioneering work on NO, Crosley and Zare[2] utilized the fortuitous overlap of a single, sharp, atomic emission line with a particular rotational transition in the molecular band structure to overcome this difficulty. Hence the upward exciting transition was exactly specified, although radiation from the downward transition was accepted over a variety of branches with consequent loss in level-crossing–signal strength.

In the present experiment we have taken a different approach. Because relatively intense OH emission in the band is easily produced (e.g., in a discharge in water vapor), we have used this radiation for the excitation process. The fluorescence is then observed through a small, fast ($f/5.3$) monochromator which isolates a single branch in the radiative decay. This technique permits a systematic study of various sublevels of the rotational band. It is limited however to molecules such as the hydrides which have an unusually coarse rotational structure, so that the necessary resolution may still be obtained with monochromator slits wide enough to avoid a crippling loss of intensity.

The specific transitions which we have measured are listed in Table I. In addition we have observed a Hanle signal for the $Q_1 1$ and the $Q_1 2$ transitions: The former is quite weak however, and the latter is complicated by the presence of the nearby $R_2 2$ line.[6] Further work is planned on these lines. For values of $K > 5$, the Boltzmann population of our OH sample drops rapidly and good signals cannot easily be obtained.

Since there are several upward branches from our resonance lamp exciting each rotational level, the net zero-field level-crossing signal is calculated to be only ~14 % under the best circumstances ($Q_1 4$ line) using linearly polarized input and output radiation. Because of the low transmission of available uv polarizers we chose to work without them, and therefore our estimated signal strength is only ~4 % of the total scattering $Q_1 4$ radiation and somewhat less for the other lines observed. These estimates are well supported by observation.

The experimental arrangement is depicted in Fig. 1 and is similar in geometry to that usually used for atomic level-crossing spectroscopy.[5] Resonance radiation to excite the $^2\Sigma_{1/2}{}^+$ state is produced by a microwave discharge in water vapor at a pressure of about 0.8 Torr. The light scattered into a 0.2-sr solid angle centered

Table I. Line designations are given in the notation of Dieke and Crosswhite (Ref. 3). $K$ is the molecular rotational quantum number and $J$ is the total angular-momentum quantum number. Relative line strengths are taken from Dieke and Crosswhite, Table 4. See text for significance of entries for calculated $g$ factors.

| Line designation | $K$ | $J$ | $\lambda$ (Å) | Relative line strength | Number of runs taken | Average experimental $g$ factor | Calculated $g$ factor |
|---|---|---|---|---|---|---|---|
| $Q_1 3$ | 3 | $\frac{7}{2}$ | 3081.54 | 25.3 | 7 | $0.176 \pm 0.023$ | $0.275^{+0.048}_{-0.037}$ |
| $Q_{21} 3$ | | $\frac{5}{2}$ | 3081.62 | 4.2 | | | |
| $Q_1 4$ | 4 | $\frac{9}{2}$ | 3083.28 | 33.7 | 11 | $0.141 \pm 0.015$ | $0.222^{+0.028}_{-0.032}$ |
| $Q_{21} 4$ | | $\frac{7}{2}$ | 3083.37 | 4.2 | | | |
| $Q_1 5$ | 5 | $\frac{11}{2}$ | 3085.20 | 42.2 | 10 | $0.118 \pm 0.011$ | $0.18^{+0.019}_{-0.016}$ |
| $Q_{21} 5$ | | $\frac{9}{2}$ | 3085.32 | 4.0 | | | |

around 90° to the incident light and magnetic field directions is analyzed by a McPherson Model No. 218 monochromator set to pass the individual $Q_1K$ lines listed in Table I. The weak adjacent $Q_{21}K$ satellite line was also passed by the monochromator in each case.[7] The slit width was 100 $\mu$ and the dispersion of 13.3 Å/mm provides a resolution of about 1 Å for all data used in determining the $g$ factors.

The OH is produced by the method described by Del Greco and Kaufman[8] in which a microwave discharge produces atomic hydrogen from $H_2$ at a pressure of ~1 Torr. The mixture of H and $H_2$ is continuously pumped through a narrow glass orifice to allow a much lower pressure in the scattering chamber, and is piped about 30 cm through carefully cleaned glass tubing to be mixed with $NO_2$ just above the scattering region. The predominant reaction is $H + NO_2 \rightarrow OH + NO$.

An EMI type 9526A photomultiplier, cooled by dry ice, is used to detect the scattered light, and a TMC multichannel analyzer in its multiscaling mode is used as a signal averager to count the output pulses of the photomultiplier as the applied magnetic field is varied. A sawtooth ramp, internally generated by the analyzer and synchronous with its channel address sweep, was used to drive the magnetic field coils through a Hewlett-Packard 6824A broad-band power amplifier. The linearity of the sweeping field was found to be better than 2 % by monitoring the voltage across a precision resistor in series with the main field coils. These coils consisted of a Helmholtz pair (see Fig. 1) with a 10-cm radius. Orthogonal compensating Helmholtz pairs were used to reduce the ambient-field components to less than about 3 mG.

The usual ramp cycle time was 10 sec per sweep of 100 channels and the typical averaging time for one "run" was about $1\frac{1}{2}$ h. A total of 28 such runs was taken, distributed over the $Q_1 3$, $Q_1 4$, and $Q_1 5$ lines. Various sweep times over the range 0.1-100 sec per sweep were used on some sample runs to check for instrumental distortion, but no changes in the signal width or shape were found.

After each run the contents of the signal averager memory were plotted by an $x$-$y$ recorder and digitized. A nonlinear least-squares program was used to fit a Lorentzian curve to the data from each run. The Lorentzian curve was augmented by the mixture of variable proportions of dispersion line shape or sloping baseline: In nearly all runs the proportion was less than 3-4 % of the signal amplitude and varied randomly in sign, indicating no consistent line-shape distortion. In any case the effect of these admixtures on the computed line width was negligible. Figure 2(b) shows a typical set of data points and the curve fitted to it. The typical uncertainty associated with the computer-determined width of the Lorentzian for each run was approximately 4 %. Uncertainty in the field strength and the sweep is about 1 %.

Figure 2(a), showing pressure broadening of the $Q_1 4$ line, indicates that pressure broadening is negligible below 1 mTorr.[9] All data used to obtain the $g$ values listed in Table I were obtained at pressures of 0.3-0.8 mTorr.

If $\tau$ is known, individual $g$ factors may be derived from our data. The $^2\Sigma_{1/2}{}^+$ state lifetime has been measured in a number of experiments as reviewed by Golden, Del Greco, and Kaufman.[10] Although earlier work shows a large spread of values, the recent results of Bennet and Dalby[11] and of Golden, Del Greco, and Kauf-

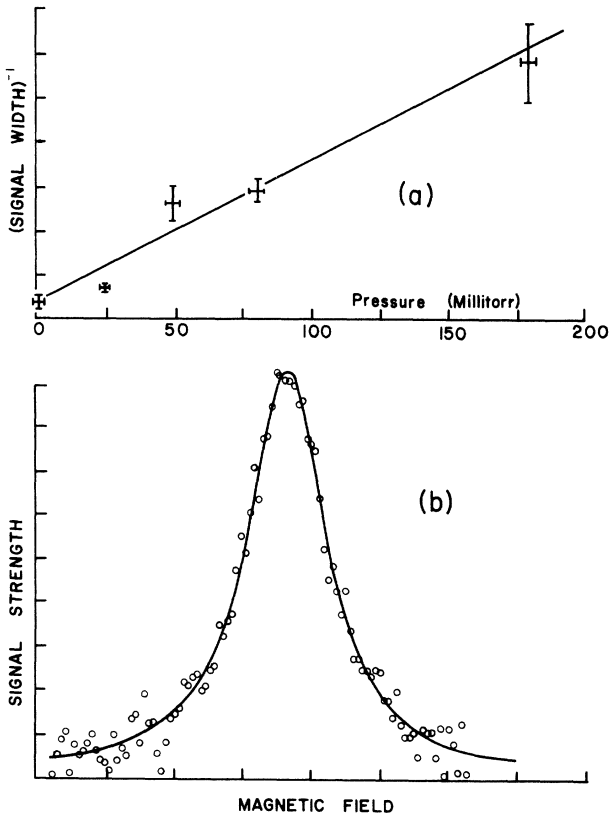


FIG. 2. (a) Reciprocal of the Hanle signal width at half-maximum (arbitrary units) versus pressure. (b) Example of typical set of data (symbols) and computer fitted Lorentzian curve. There are 100 channels uniformly distributed over approximately 4.5 G.

man,[10] obtained by careful application of two different methods, are in excellent agreement with one another. The oscillator strengths $f(Q_1 4)$ and $f(P_1 2)$ measured by Golden, Del Greco, and Kaufman, when combined with the relative line strengths for competing transitions tabulated by Dieke and Crosswhite,[4] yield independently $\tau = 1.03 \times 10^{-6}$ sec and $\tau = 1.05 \times 10^{-6}$ sec for the $K = 4, J = \frac{9}{2}$ and $K = 1, J = \frac{3}{2}$ rotational sublevels of the $^2\Sigma_{1/2}{}^+$ state. (These two sublevels should have essentially identical lifetimes, in common with the other sublevels measured here.) The above results compare very well with the value $(1.01 \pm 0.05) \times 10^{-6}$ sec determined by Bennet and Dalby. We have adopted the value $(1.03 \pm 0.05) \times 10^{-6}$ sec in computing the $g$ factors listed in Table I. The error values listed there represent the standard deviation of the widths for all runs on that particular line, added to a 1% uncertainty for the magnetic field and a 5% uncertainty for the lifetime.

Since the excited state is a $\Sigma$ state ($\Lambda = 0$), the coupling is expected to be nearly pure Hund's case (b).[12] The electronic spin is then coupled to $K$ giving rise to the $\rho$ doublet with angular momenta $J = K \pm \frac{1}{2}$. Neglecting hyperfine interaction the $g$ factors for case (b) are

$$g_{K \pm \frac{1}{2}} = \pm (K + \tfrac{1}{2})^{-1}. \quad (3)$$

The hfs modifies this by the usual factor (where $I = \frac{1}{2}$)

$$g_F = g_J [F(F+1) + J(J+1) - I(I+1)] / [2F(F+1)]. \quad (4)$$

The extreme limits of the range of $g_F$ values obtained via Eq. (4) for each hyperfine level contributing to a given line are indicated by the $\pm$ values associated with the theoretical $g_J$ values in Table I. Reference to Table I reveals a marked disparity between the case (b) values and our experimental $g$ factors. In no case does the measured value lie between the limits of predicted hfs values. Neglecting hfs for a moment, one finds that the experimental and theoretical values differ by a factor of about 0.65. Equation (3) shows that the reciprocal $g$ factors (neglecting hfs) should be linear in $K$. The difference in slope of experimental and theoretical plots for $g^{-1}$ vs $K$ may be partly due to neglect of appropriate weighting of the various hfs components in each transition, and for the same reason the excellent linearity of the experimental data for $g^{-1}$ vs $K$ must be regarded as somewhat fortuitous. However, the neglect of hfs clearly cannot account for the large relative displacement of the theoretical and experimental plots.

Though no simple coupling scheme accounts for the measured $g$ factors, they may arise from some intermediate coupling in the molecule. Even though $\Lambda = 0$ in the $^2\Sigma$ state, the rapidly precessing components $L_x$ and $L_y$ of the electronic orbital angular momentum may interact with the spin in higher approximation, and in fact Van Vleck has shown[13] that this interaction may contribute as much or more to the $\rho$ doubling than the $\vec{K} \cdot \vec{S}$ term. These contributions have the same energy dependence on $K$. In the $^2\Sigma$ state of OH the $\rho$ doubling is unusually large (>3000 MHz); so the orbital contribution may be quite large. The possibility of accounting for the $g$ factors by intermediate coupling is currently being investigated.

In the future, in addition to other Hanle-effect measurements in OH, we hope to investigate the hyperfine structure of the $^2\Sigma$ state via the high-field crossings. The signal associated with these crossings are, however, calculated to be much weaker than the Hanle signals. Alternatively, it may prove feasible to use the optical-double-resonance technique which would give more accurate $g$ factors and might provide crude measurements of the hyperfine splittings. These results may be of considerable interest in helping to elucidate the pumping mechanism which gives rise to the unusual population inversions observed in radio emission from the ground-state sublevels of interstellar OH.[3,14]

We wish to thank Dr. H. E. Radford of the National Bureau of Standards for his valuable advice on the technology of OH production.

---

*Work supported by the National Science Foundation.

[1]R. N. Zare, J. Chem. Phys. 45, 4510 (1966).

[2]D. R. Crosley and R. N. Zare, Phys. Rev. Letters 18, 942 (1967).

[3]See, for instance, M. M. Litvak, A. L. McWhorter, M. L. Meeks, and H. J. Zeiger, Phys. Rev. Letters 17, 821 (1966).

[4]G. H. Dieke and H. M. Crosswhite, J. Quant. Spectr. Radiative Transfer 2, 97 (1962).

[5]See, for instance, R. L. deZafra and W. Kirk, Am. J. Phys. 35, 573 (1967).

[6]The $P_1 1$ line, which is unresolved from the adjacent $Q_1 3$ line in our experiment, contributes no Hanle signal with our geometry, hence allowing unambiguous measurement of $Q_1 3$.

[7]The $g$ factors of the satellite lines have the same magnitude as each main line; hence they do not interfere with the measurement.

[8]F. P. Del Greco and F. Kaufman, Discussions Faraday Soc. 33, 128 (1962).

[9]Unfortunately the unknown composition of the chemical combination products in the scattering region makes it impossible to extract meaningful depolarization cross-section data from our pressure broadening measurements.

[10]D. M. Golden, F. P. Del Greco, and F. Kaufman, J. Chem. Phys. 39, 3034 (1963).

[11]R. G. Bennet and F. W. Dalby, J. Chem. Phys. 40, 1414 (1964).

[12]G. Herzberg, Molecular Spectra and Molecular Structure (D. Van Nostrand Company, Inc., Princeton, N. J., 1950), 2nd ed., Vol. 1, Chap. 5.

[13]J. H. Van Vleck, Phys. Rev. 33, 467 (1929).

[14]See, for instance, M. M. Litvak, in Interstellar Ionized Hydrogen, edited by Y. Terzian (W. A. Benjamin, Inc., New York, 1968), p. 713.

## ADIABATIC COMPRESSIONAL COOLING OF $He^3$†

R. T. Johnson, R. Rosenbaum, O. G. Symko, and J. C. Wheatley
Department of Physics, University of California at San Diego, La Jolla, California 92037
(Received 23 December 1968)

By adiabatic compression of a two-phase mixture of liquid and solid $He^3$, temperatures below 2.5 mK have been obtained. These are in the range expected for nuclear ordering in solid $He^3$.

By adiabatically compressing a two-phase mixture of liquid and solid $He^3$, we have cooled it to temperatures in the range of 2 to 3 mK from initial temperatures in excess of 24 mK. Independent evidence suggests that these low temperatures are near the ordering temperature in the solid $He^3$. The possibility for such cooling was suggested by Pomeranchuk[1] and qualitatively demonstrated by Anufriyev,[2] who obtained a low temperature below 20 mK with a starting temperature of 50 mK. The present low temperature is the lowest ever obtained by purely mechanical means.

Only a few remarks on experimental method will be given here. The $He^3$ cell consists of two interconnected parts: a flexible-walled metal cell of special design[3] which has elastic characteristics such that it can support pressure differences in excess of $P_{min}$, the minimum melting pressure of 28.9 atm, and a rigid-walled epoxy cell. We have 0.5 g of powdered cerium magnesium nitrate (in a right circular cylinder with diameter equal to height) for thermometry[4] at the bottom of the rigid section and in the $He^3$. Outside the flexible section is pure liquid $He^4$, which may be pressurized to as much as 25 atm (367 lb/in.$^2$), to compress the $He^3$. For precooling, the above device is sealed into a specially designed mixing chamber for our dilution refrigerator.[5] Owing to high thermal resistances, mainly boundary resistance, precooling is slow but thermal isolation is correspondingly good once compressional cooling has begun.

In practice, because of plug slippage problems in the $He^3$ filling line, the $He^3$ is precooled to about 100 mK and then, with zero $He^4$ pressure, the plug is formed. After further precooling the $He^4$ is pressurized, usually at a rate of about 1 lb/in.$^2$ min. Results for two runs are shown in Fig. 1. Starting at the lowest $He^4$ pressure indicated for a given run, there is a slight cooling with increasing $He^4$ pressure due to the negative expansion coefficient[6] of liquid $He^3$. There is a sudden increase in the cooling rate when solid $He^3$ begins to form. The temperature then falls steadily into the low millikelvin range. Particu-

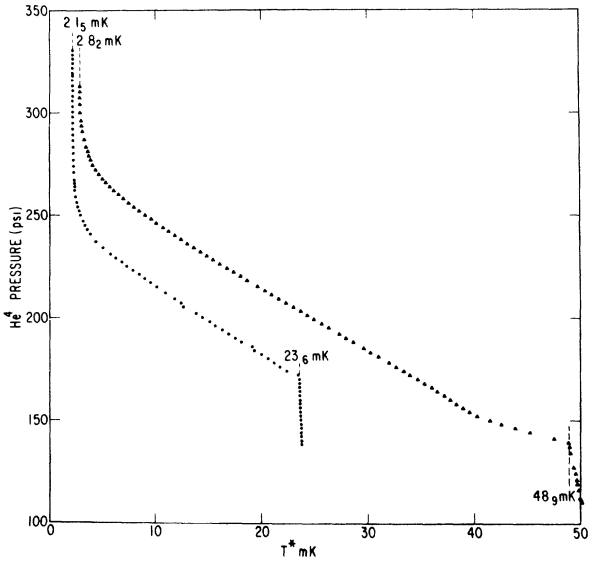


FIG. 1. Dependence of $He^3$ temperature, as indicated magnetically with cerium magnesium nitrate, on the pressure of liquid $He^4$ used to compress the $He^3$.